Hybridization of Guided Surface Acoustic Modes in unconsolidated granular media by a resonant metasurface

Supplemental Material

Antonio Palermo[1,5], Sebastian Krödel[2], Kathryn H. Matlack[2,3], Rachele Zaccherini[4], Vasilis K. Dertimanis[4], Eleni N. Chatzi[4], Alessandro Marzani[1], Chiara Daraio[5*]*

[1]Department of Civil, Chemical, Environmental and Materials Engineering - DICAM, University of Bologna, Bologna, Italy

[2]Department of Mechanical and Process Engineering, ETH Zürich, Zürich, Switzerland

[3]Department of Mechanical Science and Engineering, University of Illinois at Urbana-Champaign, IL

[4]Dept. of Civil, Environmental and Geomatic Engineering, ETH Zürich, Zürich, Switzerland

[5]California Institute of Technology, Division of Engineering and Applied Science, Pasadena, CA

*Corresponding author: *daraio@caltech.edu; *alessandro.marzani@unibo.it.*

Experimental setup details

The experimental setup has been built in the IBK Structures LAB at ETH Zurich. The wooden crate that supported the granular medium for the experiments was filled with glass beads for a total mass of approximately $3800\,kg$. The glass beads were gently deposed in small amounts, i.e. packages of $25\,kg$. The bottom surface of the box was covered with a 2-mm-thick paperboard plate to reduce wave reflections, as suggested in Ref. [18].

We excited the granular medium surface using an $8\,mm$ diameter metallic rod of length $250\,mm$ inclined of $20\,deg$ with respect to the vertical direction, as suggested in Ref. [18] for a similar setup. The metallic rod was attached to an electromagnetic shaker (Tira, Vibration Test Systems N1000 to N2700), driven by a waveform generator (Agilent, 33220). We recorded (with a sampling rate of 500 kHz) the surface vertical velocity using a laser Doppler vibrometer (Polytec, OFV-500) and used a thin layer of reflective glass powder (Glasperlen, diameter of 150-250-μm) along the line measurement to maximize the laser signal quality (Fig. S1a). At each acquisition point, we averaged 32 signals to reduce the signal to noise ratio. All instruments were controlled using a MATLAB© interface.

GSAM phase velocity

The velocity wavefield recorded along the symmetry axis of the box and used to trace the seismograph in Fig. 1b was transformed into the frequency-phase velocity domain using a slant

stack transform (see Fig. S1b). In the frequency phase-velocity domain, the two distinct slowest P-SV waves were identified and labelled N_1 and N_2. They traveled with phase velocities $c_{p,1} = 35 - 60\ m/s$, $c_{p,2} = 60 - 90\ m/s$ within the frequency range $250 - 650\ Hz$.

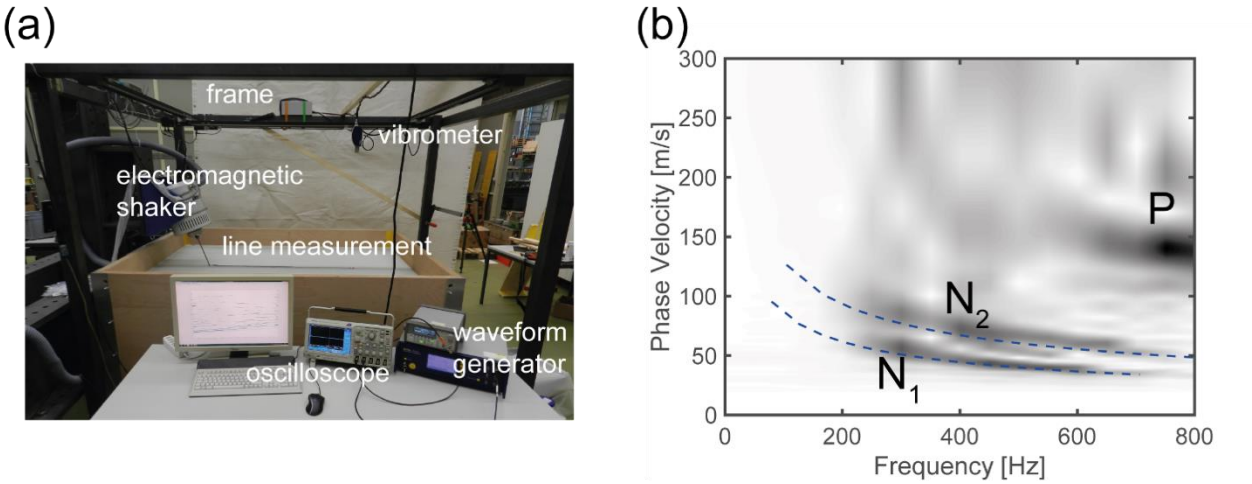

Figure S1 (a) The experimental setup. (b) Frequency phase-velocity plot of the velocity wavefield recorded along the symmetry line of the box. Dashed blue lines mark the phase velocities of modes N_1 and N_2 as predicted according to the GSAM theory developed in Ref [17].

3D Printed Resonators

The 3D printed resonators consisted of a rigid cylindrical shell (height $24\ mm$, external diameter $20\ mm$, thickness $1.2\ mm$), where a cylindrical steel mass (height $12\ mm$, diameter $12\ mm$) was encased, supported by a truss-like spring. The cylindrical shell and the truss-like spring were both printed in Acrylonitrile Butadiene Styrene (ABS) (see Table S1 for material properties and Fig. S2a for the detailed geometry). The truss-like spring was composed of 16 trusses (length l, cross-section $1.2x1.2\ mm^2$) arranged in a cross like configuration with a relative inclination angle α in the vertical plane.

By varying the truss length and relative angle α within the limit imposed by the dimension of the rigid cylindrical shell and ensuring subwavelength dimension of the resonator along the depth (overall height <$25\ mm$), the first resonator vertical resonance can be easily tuned over a wide range of frequency (for example 250 Hz-700 Hz). We guide the design of the resonator geometry using a 3D FE model developed in Comsol Multiphysics©, calculating the resonator natural frequencies, assuming fixed boundary conditions at the base of the cylindrical shell.

With a truss length $l = 5.75\ mm$ and an angle $\alpha = 65$ deg, the resonators had a first vertical frequency of approximately $500\ Hz$ (see Fig. S2a), confirmed experimentally by testing selected resonators.

We embedded the resonators in the granular medium and tested their response when subjected to a surface Ricker wavelet excitation. The embedded resonators had a measured first vertical

resonance frequency $f_r = 410\,Hz$ (see Fig.S2b). The discrepancy between the natural and embedded frequency results from the presence of the soft granular medium surface layer which acts as a further soft spring at the base of the resonator.

Table S1 3D printed resonator material properties

Material	Young modulus	Poisson ratio	Density
Steel	$E = 210\,GPa$	$\nu = 0.3$	$\rho = 7800\,\frac{kg}{m^3}$
ABS	$E = 2.5\,GPa$	$\nu = 0.3$	$\rho = 1400\,\frac{kg}{m^3}$

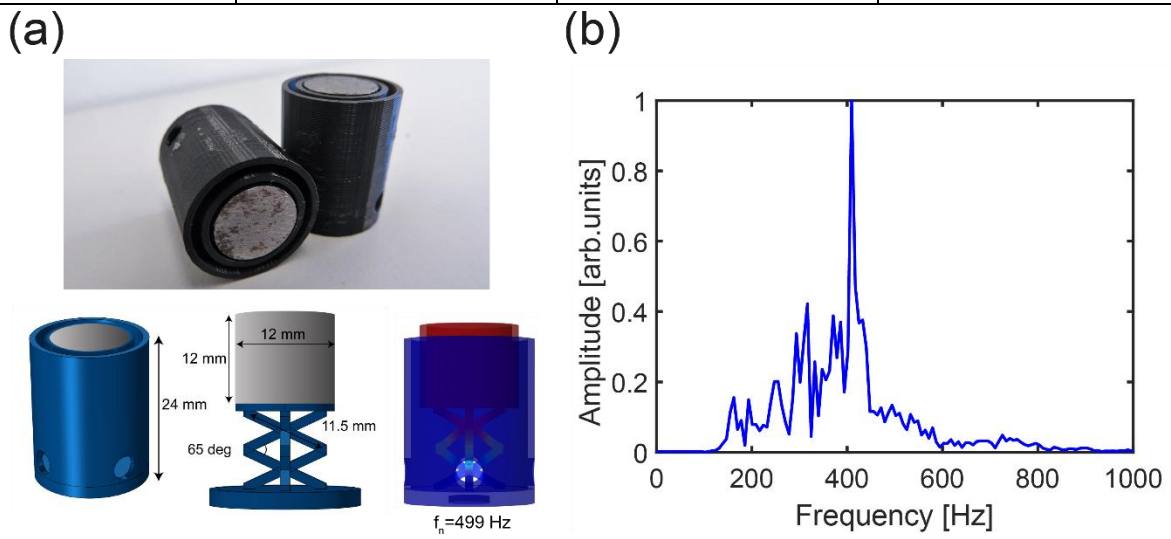

Figure S2 (a) The 3D printed resonator. Geometry and calculated first natural frequency. (b) Measured frequency response of a 3D printed resonator buried in the granular medium surface.

FE models

Real size experimental setup

We develop a FE model of the experimental setup in Comsol Multiphysics©, which simulates the propagation of a Ricker pulse along the measurement line. To this aim, we model the granular medium in plane strain conditions, assuming the power law stiffness profile $c_{S,L}(z) = \gamma_{S,L}(\rho g z)^{\alpha_{S,L}}$ reported in Ref. [17]. The geometry of the model reproduces exactly the middle plane of the wooden box filled up with granular beads with a chain of 20 2D resonators (see Fig.S3(a)). Each 2D resonator has an equivalent 2D mass, calculated alike to the truss-mass resonator. The source is modelled as a Ricker point force, inclined of $20\,deg$ with respect to the vertical direction and applied at a depth $h_{source} = 0.015\,m$. Low reflective boundaries are used to minimize the reflections.

We model the propagation of a Ricker pulse in the granular medium with and without (free field condition) surface resonances. For the free field condition, we use the surface vertical displacement field calculated over a grid of 500 points along a line of 1 m starting from the source to reconstruct the seismograph of the Ricker pulse (see Fig. S3(b)). The 2D Fourier Transform of the displacement wavefield (Fig. S3(c)) provides an $f-k$ spectrum, which is in excellent agreement with the experimentally derived spectrum of Fig. 1(c). For the surface resonance case, we calculated the displacement field over the same grid and evaluated the $f-k$ spectrum (Fig. S3(e) using the wave field data over the chain of resonators, analogously to the experimental $f-k$ spectrum (Fig. 1e). As for the experimental case, the numerical simulation provides a clear evidence of the hybridization of the lowest P-SV wave with the surface resonances, without significant insight on the higher frequency range.

Large size model

The large size 2D FE model is based on the same assumptions (i.e., plane strain conditions, granular medium with power law stiffness profile, truss-point mass resonators) of the unit cell model. The time transient simulations are calculated for a time window of $400\,ms$ with a time step $dt = 0.05\,ms$. The $f-k$ spectrum of the wavefield of the surface resonant region (Fig. 4(b)) is calculated over a length of 8 m with a grid of 800 points (see Fig. S4(a)). The $f-k$ spectrum of the displacement field of the reflected waves (Fig. 4(a)) is calculated over a length of 5 m with a grid of 250 points. Fig.S4(b) displays the $f-k$ spectrum of the displacement field after the resonant region calculated over a length of 4 m with a grid of 200 points (Fig. S4(a)). This spectrum confirms that after the resonant region the wavefield is completely recovered, i.e., no energy leakage is induced by the surface wave delocalization. Mode N_1 is however characterized by a slightly weaker energy trace in the low frequency range ($f < f_r$) due to the amount of energy back reflected or trapped by the resonators near the resonance.

FE mesh and time stepping

We remark that all the results extracted via FE simulation are obtained with convergent meshes of quadratic elements, with at least 6 elements along the direction of wave propagation for the shortest wavelength. For all the time transient simulations, we use an unconditionally stable time integration scheme (generalized alpha scheme), with a time step $dt > 10\,f_{max}$, where f_{max} is the maximum frequency considered.

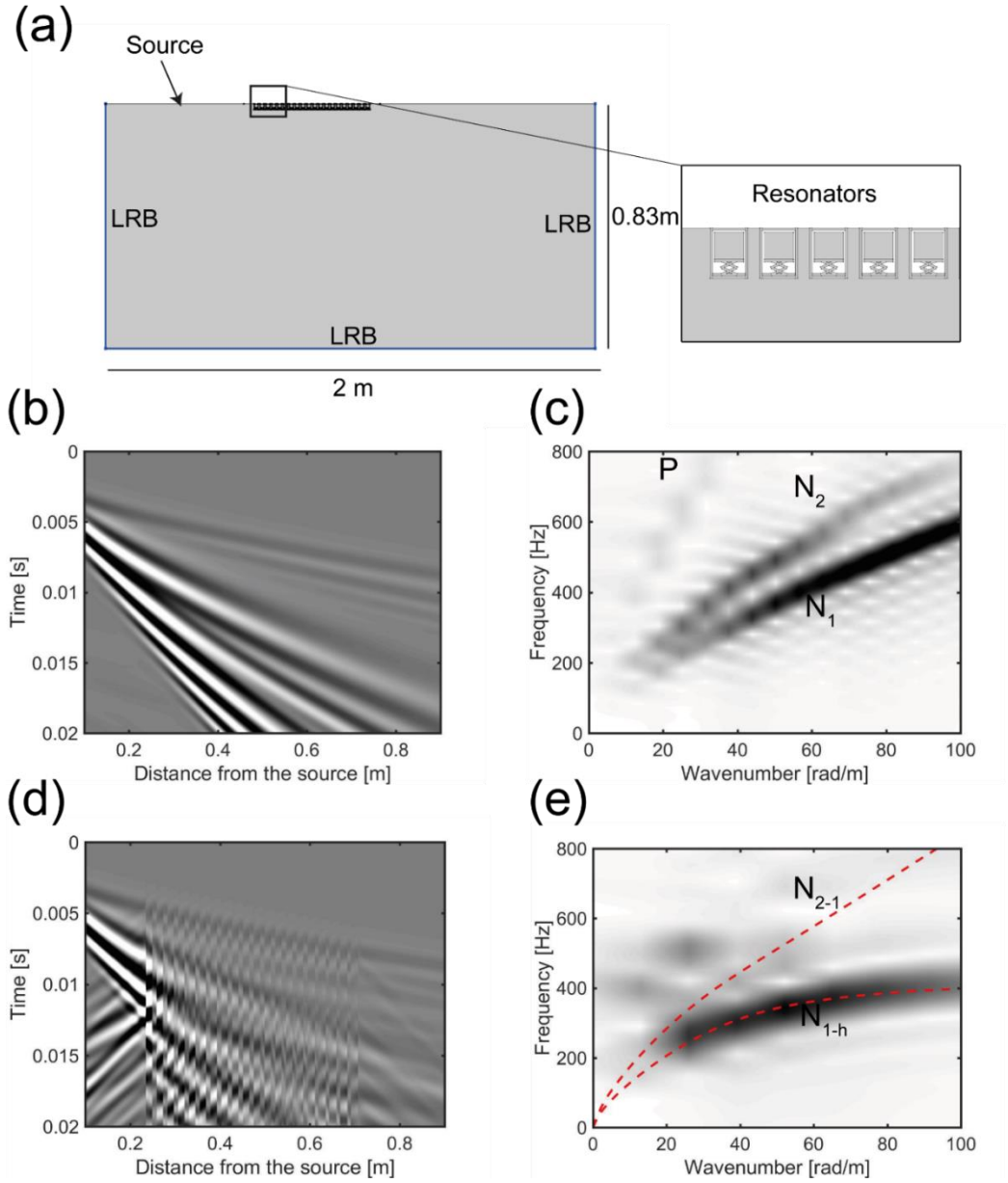

Figure S3 Numerical simulations of GSAMs interacting with surface resonances. (a) Geometry of the 2D FE model (b) Seismograph of a Ricker pulse propagating in the granular medium. (c) Dispersion curve of low order GSAMs travelling in the granular medium: the gray color map is the 2D Fourier Transform magnitude of the numerical seismograph. (d) Seismograph of a Ricker pulse propagating trough the surface resonances embedded in the granular medium. (e) Dispersion curve of low order GSAMs interacting with surface resonances: the gray color map is the 2D Fourier Transform magnitude of the numerical seismograph, while the dashed-red curves indicate the lowest order modes ($N_{1\text{-}h}$, $N_{2\text{-}1}$) calculated from the unit cell numerical model.

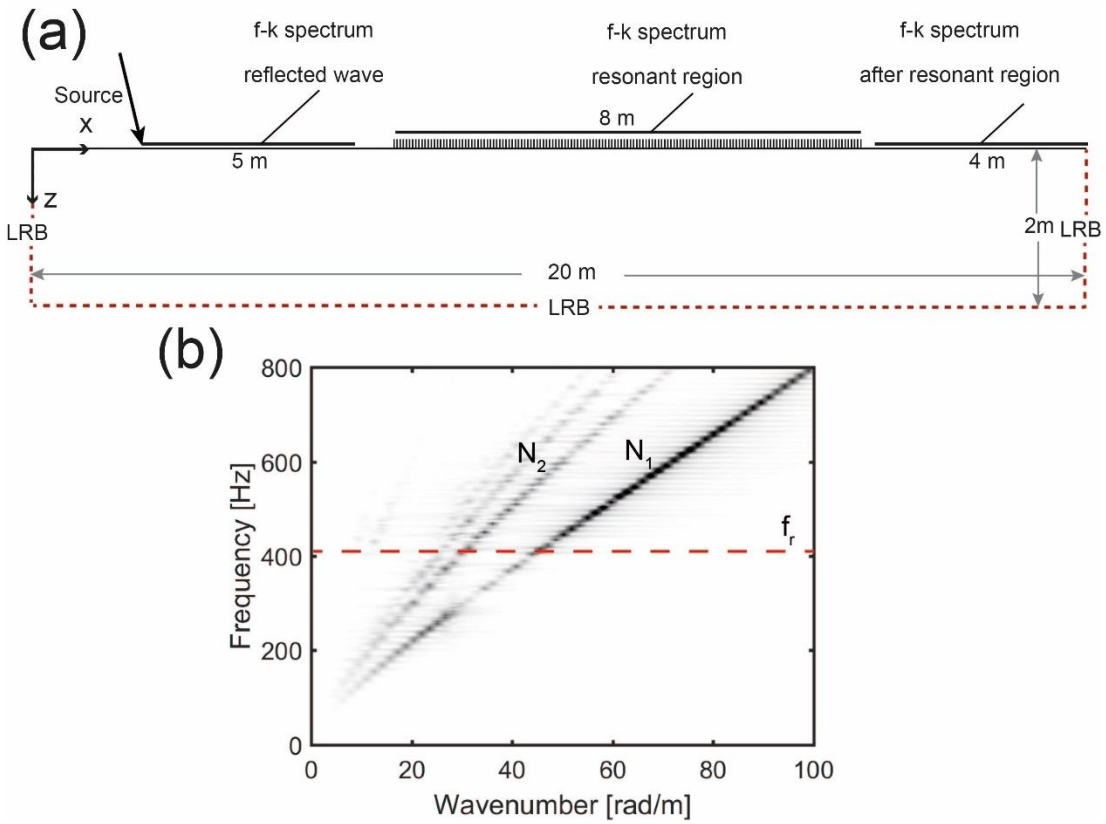

Figure S4 (a) Details of the2D FE numerical model. (b) Dispersion curve of the surface wavefield after the resonant region.